Mechanical excavation of clayey soils, a review of the physical phenomena occurring

Winkelman, M.O.; Schott, D.L.; Helmons, R.L.J.

Publication date
2024

Document Version
Final published version

Published in
Proceedings CEDA Dredging Days 2024

Mechanical excavation of clayey soils, a review of the physical phenomena occurring

Winkelman, M.O.; Schott, D.L.; Helmons, R.L.J.

Publication date
2024

Document Version
Final published version

Published in
Proceedings CEDA Dredging Days 2024

MECHANICAL EXCAVATION OF CLAYEY SOILS, A REVIEW OF THE PHYSICAL PHENOMENA OCCURRING

M.O. Winkelman[1,2], D.L. Schott[3] and R.L.J. Helmons[4]

Abstract: Clay is a notoriously challenging material to dredge. Due to its adhesion and plastic behaviour, it may clog the suction head of a dredge and clay balls could form down the pipeline. This will raise difficulties in estimating the production or the required power and increases the risk of downtime. As this is important for the dredging industry, there is a lot of literature on the cutting of clay in dredging, mostly it focused on the forces and stress distribution near the blade tip. Unfortunately, there is little information on the influence of adhesion and plasticity of clay on the deformation and the sliding of the clay chip over the tool and their contribution to the total cutting forces. Existing models on clay cutting are likely to miss some key details of clay behaviour.

This paper, summarizes published results from experiments of cutting in clay. The results uniformly evaluated with dimensionless parameter groups derived by the Buckingham Π method. These Π groups can be used as characteristic numbers to investigate trends. The state of the art of models for cutting highly plastic materials is presented, providing a more detailed description of the excavation processes in submerged clay. The test results have been compared with the existing models. This provides insights regarding chip formation and the deformation of the chip as it moves along the tool. That knowledge provides a basis for solutions needed to avoid clogging of equipment and the occurrence of clay balls. In the next phase of the project, the identified Π groups will be used for the selection of the operational settings causing tear type cutting which leads to the break up of the chip into balls.

This review is part of the CHiPS project, which investigates rapid large plastic deformations in submerged clay for Cutting Highly Plastic Soils.

Key words: Clay cutting, Plasticity, Adhesion/cohesion ratio, Deformation types, Chip formation

[1]Delft University of Technology, the Netherlands, m.o.winkelman-1@tudelft.nl
[2]Damen Dredging Equipment, the Netherlands, Mark.Winkelman@damen.com
[3]Delft University of Technology, the Netherlands, d.l.schott@tudelft.nl
[4]Delft University of Technology, the Netherlands, r.l.j.helmons@tudelft.nl

1 INTRODUCTION

Whenever clay is encountered in a dredging project, it may cause several problems for the operator of the dredging equipment. The shear strength may be very high, and consequently, the required power to remove it will increase or conversely the production will be reduced. Or, the plasticity and adhesion are very high and the clay will stick to the equipment, not release to the suction mouth and completely cover the cutter head (see Figure 1.). Further down the pipeline, the broken chunks of clay may form clay balls, when the plasticity is high and there is sufficient sand content (Hoff and Kolff, 2012).

Figure 1. Example of using a cutter head in a highly plastic clay

The underlying processes, which cause these problems, are related to the actual cutting of the clay, the transport of the chip over the tool and the release of the chip into the suction mouth. All of which have a relation to clay plasticity and its influence on the deformation along the concerned interfaces of this chip. Both theoretical and experimental research has been carried out on the deformation process. More knowledge is available on deformation of metals and plastics, less so on the deformation of clay during cutting. To investigate the available knowledge on this deformation process an initial literature review has been performed on dredging clay and plastic deformation in this process.

Plastic deformation is a non-reversible process in response to applied forces. During the process, the internal structure of the material is changed, and the object transforms to a new overall shape. Basically, existing literature focusses on either the macro deformations, the micro deformations or the cutting types. Regarding the specific cutting process in dredging, there are several aspects to be distinguished:

- Understanding the application of cutting in dredging
- Describing the cutting types of saturated submerged clay
- Plastic deformation in general and of clay in particular
- Shear models for local deformation of the material
- The operating range for various dredging equipment in dimensionless parameters

The most relevant publications for these aspects will be presented in this paper.

2 BACKGROUND

This literature review is part of a PhD project (CHiPS: Cutting of Highly Plastic Soils) to investigate the cutting behaviour of saturated clay for dredging applications. This literature survey acts as the basis for an improved model describing the cutting behaviour. Currently, the literature review is being finalized and an experimental test facility is being developed to enable additional cutting experiments to fill in the identified knowledge gaps.. Calculating the required cutting power for dredging equipment has been a difficult exercise for a long time. An academically correct calculation requires a serious desk study. In the field, empirically derived rules of thumb seem sufficient for their purpose. As Leendert Volker stated: ‘The calculations performed here are only intended to serve as a guide for preparing the graphs for the equipment available. If one reviews a dredge this way on a lost winter evening, one will enjoy it during busier times.’ (Volker, 1947). His pragmatic recommendation is to equip a Cutter Suction Dredge (CSD) with a cutter drive of 50% of the power of the pump and a speed in the order of 10 to 15 rpm. Since then, numerous articles have been published on the calculation of cutting forces.

The World Association for Waterborne Transport Infrastructure has released a guideline on the classification of soil and how to handle them (PIANC, 2016). The recommendation starts out on the cohesiveness of soil (see Figure 2.). When soil does not have any cohesion, it can be dredged completely hydraulically. The production in loose soil can be increased by a dredge with a certain mechanical action, the extra mechanical contact will require more force and consequently will be less efficient. On the other side of the soil spectrum is strong rock. Only the most powerful CSDs will be able to engage in this material. Other equipment can only be applied when intact rock has been disintegrated by pre-treatment. Specifically, either by blasting, crushing or chipping with a drum cutter. Depending on the size of resulting fragments, the secondary material can be dredged by any other equipment that is able to collect the fragmented material. Once the cohesion in the soil is determined, specific dredging equipment can be selected, taking into account the operational boundary conditions and preferred efficiency, resulting in the amount of mechanical power the equipment will be employing.

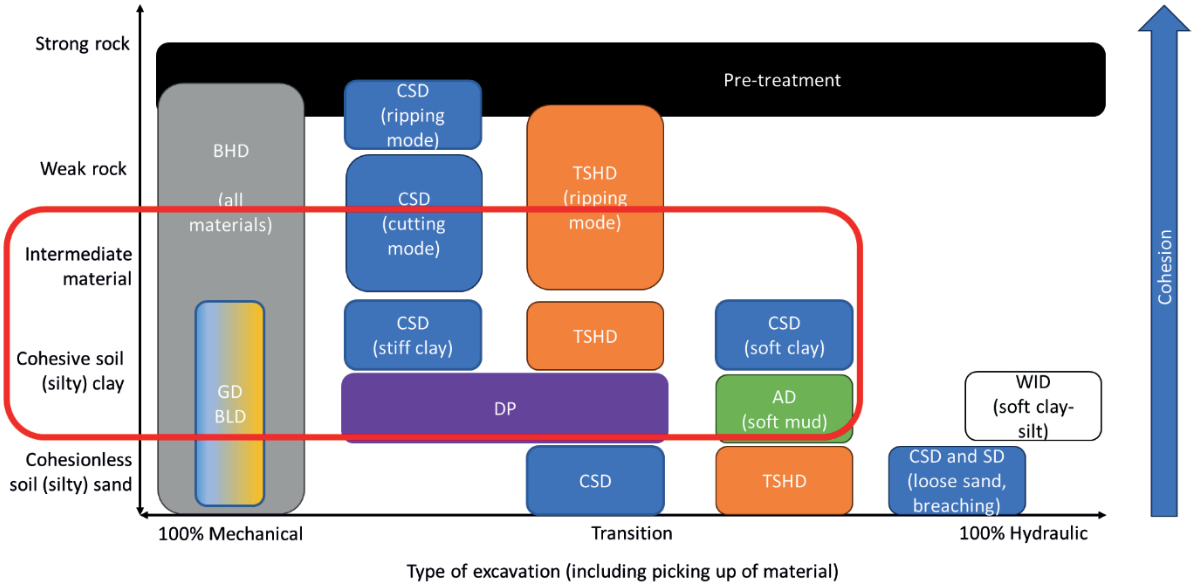

Figure 2. Dredging equipment and their applications (Based on PIANC 2016)

The PIANC recommendation (Figure 2.) for removing clay and similar, intermediate cohesive material that shows cohesion, is to select the following equipment: Grab Dredge (GD), Bucket Ladder Dredge (BLD), Back Hoe Dredge (BHD), Auger Dredge (AD), Cutter Suction Dredge (CSD) or a Trailing Suction Hopper Dredge (TSHD). Dredge Ploughs (DP) and Water Injection Dredges (WID) can also be used for very soft low cohesive soils. However, both DP and WID are often constrained by turbidity restrictions. The recommended dredge types belong to the main branch of the family of dredging equipment: the 'mechanical dredges' and the 'mechanical-hydraulic dredges' (CEDA/IADC, 2018). The material showing problematic behaviour is cohesive soil and intermediate material. It starts with highly plastic and goes over to partly brittle. The equipment highlighted in the red box in Figure 2. is most likely to encounter the processes of most interest for this research, as it aims to provide a theoretical basis for such recommendations.

3 PLASTIC DEFORMATION

3.1 Plastic deformation in general and of clay in particular

Plastic deformation is a phenomenon observed as an irreversible change in the geometry of a continuum shape at the outside due to an applied external force. The actual mechanism that is allowing this deformation on the inside of the object depends on the material itself. Crystaline materials including metals rearrange their atoms in the structure by dislocation in the crystal lattice. Even brittle materials exhibit some form of plasticity showing slip at the microcracks. In composite materials e.g. foam and tissues, the plastic deformation is mainly a consequence of rearrangement of its elements; bubbles, cells, fibres. The rearrangement at a microscale occurs by sliding or slipping of the concerned elements, crystals, bubbles, cells etc, along a linear trajectory or a continuous surface. The driving mechanism that moves these elements over or along each other is the shear stress. The orientation of the shear line or plane depends on the local stress conditions.

As stress conditions change, for each location within the concerned geometry, the orientations of the shear line changes. Aligning all these incremental shear lines after each other constructs an array of shear lines, see Figure 3. Usually they appear curved but under certain conditions they may form straight lines, e.g. under symmetrical conditions.

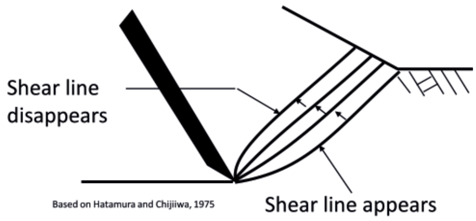

Figure 3. Appearance of shear lines, (Hatamura and Chijiiwa, 1975).

The array of shear lines was already observed (Hatamura and Chijiiwa, 1975). An array of shear lines could be calculated by the slip-lines-method (Dewhurst and Collins, 1973) as proposed by (Schoonbeek et al., 2006). Nonetheless, this has been neglected by (Miedema, 1992) in his view on cutting of clay . He assumed a straight shear line model over a unit width for ease of calculation. For calculating the total deformation force on the object, the shear stress along the shear lines must be integrated in magnitude and orientation over the area defined by the length of the shear line and the unit width. This shear stress depends on the shear rate along the shear line, and that in turn determines the geometry and the speed at which the deformation is happening. Various models for determining the shear rate on these shear lines will be discussed in section 3.2.

The plastic deformations in clay are mostly due to the rearrangement of clusters of grains. The freedom to move these clusters in their environment is limited by the space around them and thus the water within the clay structure. Plasticity in clay depends on the water content in various conditions. The critical conditions are in order of stiffer material: liquid limit, plastic limit, shrink limit, dry limit. Commonly referred to as the Atterberg Limits (see Figure 4.) (ISO 17892, 2018).

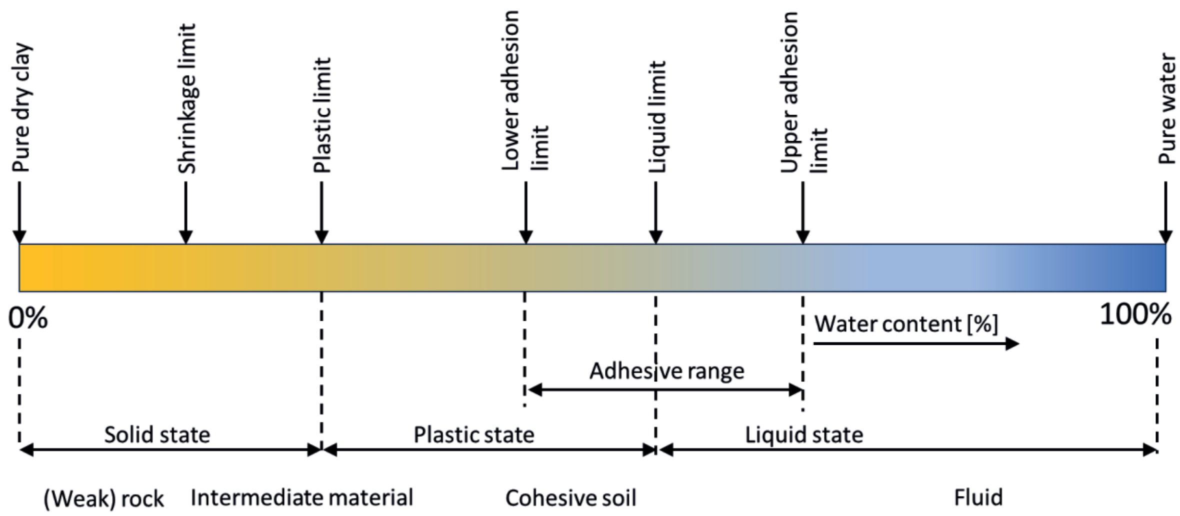

Figure 4. Atterberg Limits

As this review focusses on the plastic state of clay, the defining limits are the liquid limit (LL) and the plastic limit (PL). In the plastic state, the consistency of clay ranges from almost liquid to intermediate material that is partly brittle and partly plastic. When the water content exceeds the liquid limit and starts to flow below a certain yield strength, the clay can better be described as a fluid (Meshkati et al., 2021). When there is less water than the shrinkage limit, the clay behaves as a brittle elastic solid. Both conditions have little relevance to the problems with mechanical excavation of submerged clay. The plasticity index (PI) indicates the plastic potential of a clay, which is described as the range of water content between the liquid limit and the plastic limit. The plastic limit depends on the material itself and is independent of actual water content. The Liquidity Index (LI) indicates at which water content, relative to the Plasticity Index (PI), the material currently is.

3.2 Shear models for the local deformation of the material

Along the shear lines of the deformation field, shearing of the material generates stresses. Integrating these stresses over the areasof the slip surfaces and adding up the contributions in the various directions, provides the overall forces required for this deformation. The stresses depend on the strain, and the strain rate, during the local deformation process. This strain rate effect can be modelled in various ways, ranging from an empirical approach to a more detailed and elaborated model, see Figure 5.

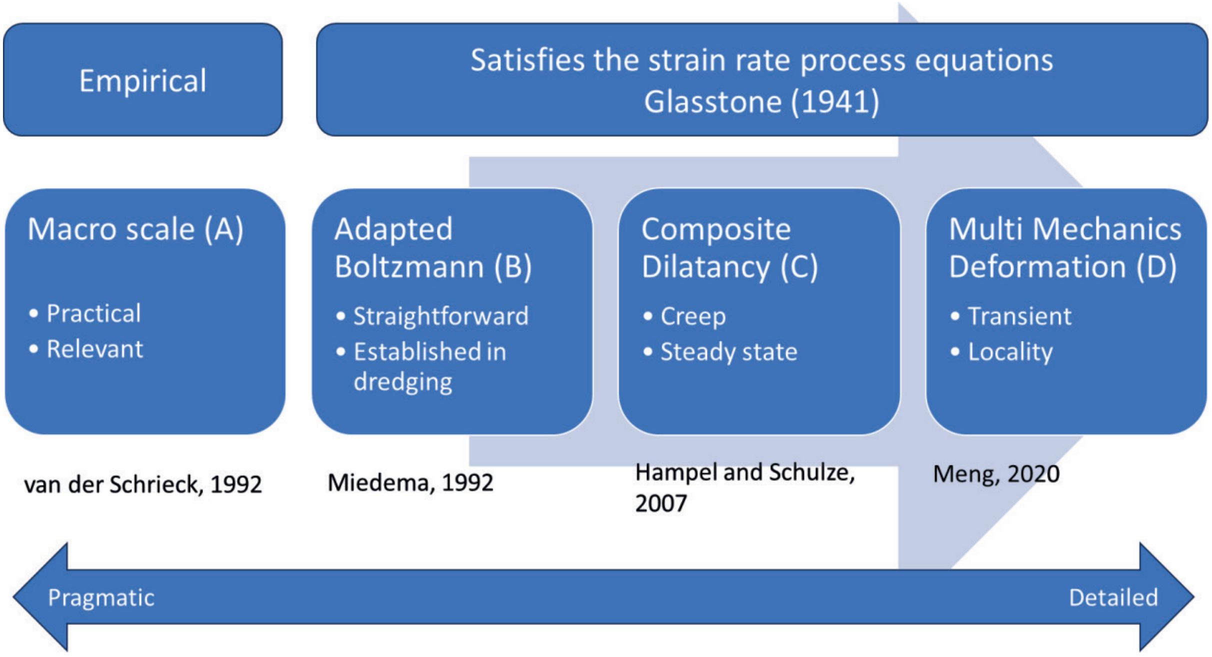

Figure 5. Strain rate process models. A,B,C and D below

Macro scale derivation (A)

As the shear rate on a micro scale is hard to measure or model, the best assumption is to relate it directly to the macro scale deformation. Such a model has been proposed (Merchant, 1941), for metal cutting. Subsequently this has been used by e.g. (van der Schrieck, 1996), to adapt it to clay cutting. This deformation rate as proposed (van der Schrieck, 1996) is a process description on macro scale. This does not yet describe actual behaviour of plastic material at the shear plane. He merely hints at the relationship between the deformation rate (cutting speed v_c over initial cutting height h_i) and the shear rate (Schrieck, 2022).

$$shear\ \dot{rate} = \varepsilon_0 = \frac{d\beta}{dt} :: \frac{v_c}{h_i} = deformation\ rate \qquad (1)$$

Problematic in this proportional relationship is that it is empirically derived from an unknown clay composition. The only parameter provided was the cohesion that apparently scales linearly. When the blade angle α changes, or the resulting shear angle β shifts, the relationship is broken. Only when working in similar conditions, the proposed graph (Figure 6.) is usable. Apparently, it was good enough to relate to practical experience of dredge operators, which is also referred to in the standard textbooks of the VBKO (VOUB, 1998).

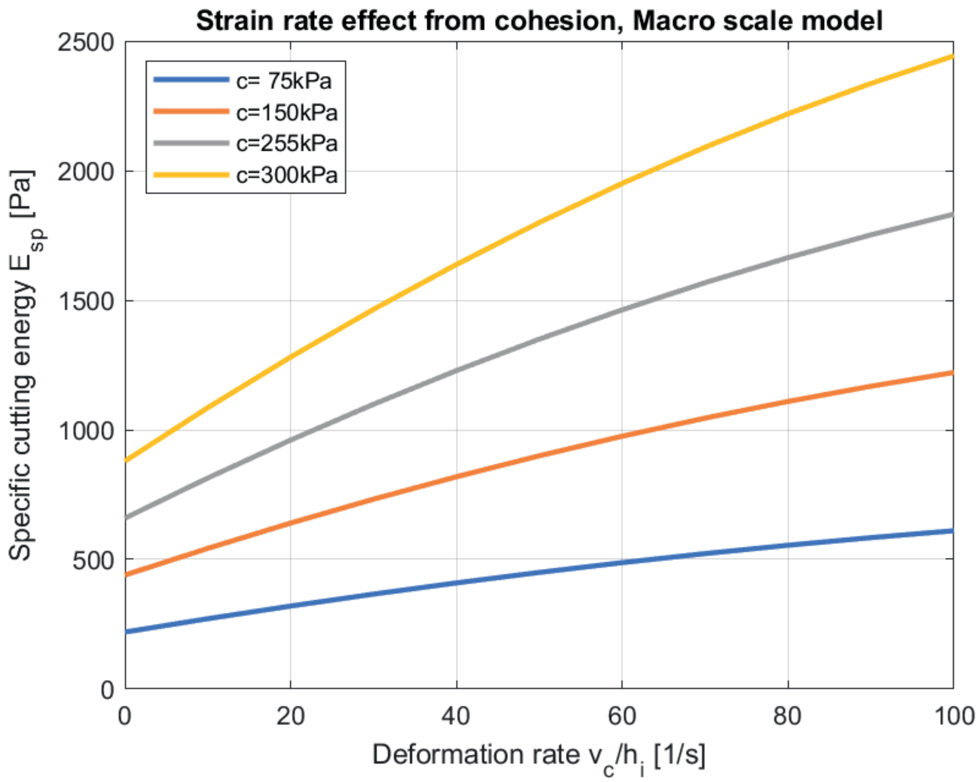

Figure 6. The strain rate effect from cohesion, the macro scale model by (Schrieck, 1996)

Rate process theory (B)

Another widely accepted model for the shear rate estimation in clay deformation is proposed by (Miedema, 1992) see, Equation 2.

$$\dot{\varepsilon}_0 = 2X\frac{kT}{h}e^{\frac{-E_a}{RT}}\sinh\left(\frac{\tau\lambda N}{2SRT}\right) \quad with: R = Nk \tag{2}$$

In this equation, the strain rate $\dot{\varepsilon}_0$ is depending on the barrier crossing function X, the Boltzmann constant k, the temperature T, the Planck Constant h, the activation energy E_a, the Universal Gas constant R, the shear stress, the distance between equilibrium points λ, Avogadro's number N and the number of bonds per unit area S.

With the resulting strain rate, the strain rate factor λ_s can be calculated:

$$\lambda_s = \left(1 + \frac{\tau_0}{\tau_y} ln\left(1 + \frac{1.4\frac{v_c}{h_i}\frac{sin(\alpha)}{sin(\alpha+\beta)}}{\dot{\varepsilon}_0}\right)\right) \tag{3}$$

Here the material properties of dynamical shearing resistance factor τ_s and the yield strength for shearing τ_y are related to the operational properties. And this will enable the calculation of the specific cutting energy E_{sp}.

$$E_{sp} = \lambda_s c\left(\frac{sin^2(\alpha)+rsin^2(\beta)}{sin(\alpha+\beta)sin(\alpha)sin(\beta)}\right) \tag{4}$$

The resulting specific cutting energy, according to this model has a different characteristic than the Macro scale model by (Schrieck, 1996) previously discussed (see Figure 7.).

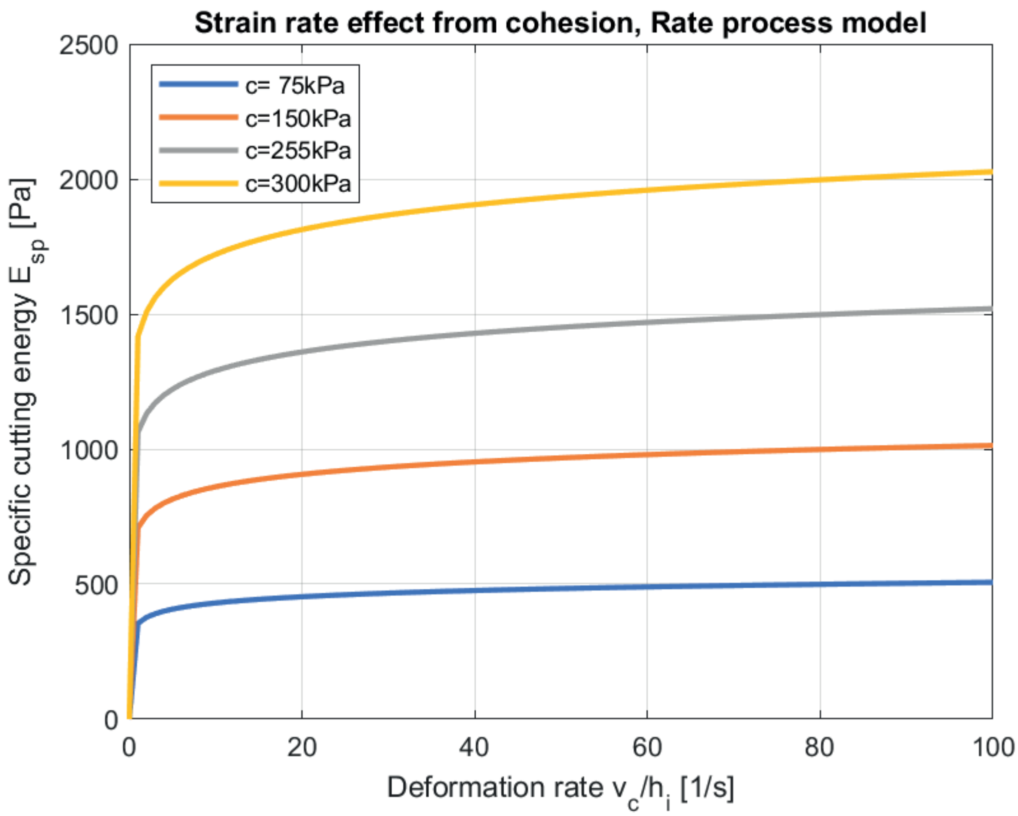

Figure 7. Strain rate effect from cohesion, the rate process model by Miedema (1992)

In principle, this model is an adaptation from the rate process theory. The rate process theory was developed by (Glasstone et al., 1941). In turn based on observations of chemical reactions in sugar molasses by (Arrhenius, 1889),and derived the chemical reaction speed as in Equation 5:

$$\varrho_{t_1} = \varrho_{t_0} e^{\frac{q(T_1 - T_0)}{2T_1 T_0}} \quad with\colon \frac{q}{2T_0} = \frac{-E_a}{R} \tag{5}$$

Here, ϱ_{t0} is the reaction rate at the initial temperature T_0 and ϱ_{t1} the reaction rate at the terminal temperature T_1. The heat consumption q for the reaction is depending on the activation energy E_a and the universal gas constant R. Arrhenius himself already simplified his model with the assumption that reacting particles are always moving head on, in a linear motion. This simplification has been adopted by Miedema. The linear motion is captured in the single factor E_a and consequently q.

Composite dilatancy (C)
This is a proposed model for shear rate in the deformation of salt masses (Hampel and Schulze, 2007). In this model, the required energy for molecular movement also uses the Boltzmann model but accounts for the non-linear movement and spatial distribution of the particles. In a sense, this is another branch from the (Glasstone, 1941) equations. Due to the non-linear movement, it accommodates a memory for the deformation allowing for hysteresis. This might be useful for calculating the shear stress on subsequent slip lines as a clay chip passes over the blade.

Multi mechanisms deformation (D)
Another adaptation of the rate process theory model is to attribute physical dimensions to the reacting particles and to extend this to the adjacent particles (Meng et al., 2020). This has been explored with the description of multi-mechanisms deformation. Next to the Boltzmann distribution, non-linear movement and spatial distribution, it accounts for different interactions between different components in clay: small and large particles, water and contaminants. The resulting model is capable of accommodating the physical dimensions of clay particles and the fluid mechanics of pore water. Though achieving this accuracy requires extra effort and will result in an adaptation of the Boltzmann distribution.

3.3 Cutting of saturated submerged clay

The cutting action has been investigated thoroughly, with models (Miedema, 2014) of various levels of accuracy. The subsequent mixture forming has seen some attention also (den Burger, 2003; Werkhoven et al., 2018). There is less literature available on the transition of the chip into the mixture. Any tugging forces induced on the attached part, will be transferred to the chip on the blade by constitutive equations. However, in most literature, these forces are neglected (see Figure 8.).

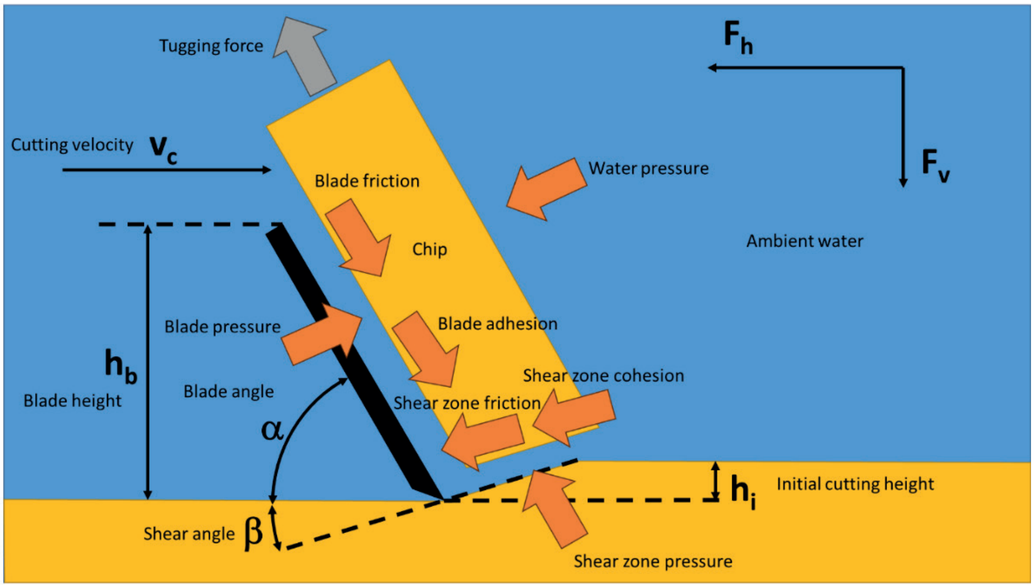

Figure 8. Generalised situation of clay cutting in dredging literature (Miedema, 1995).

4 OCCURRING CUTTING BEHAVIOUR

Due to the stress conditions arising from the cutting action, the material in front of the blade will either slide or break. (Hatamura and Chijiiwa, 1975) already identified three different cutting behaviours: Flow type, shear type and tear type, see Figure 9. Although they observed some other cutting types as well, they did not describe them.

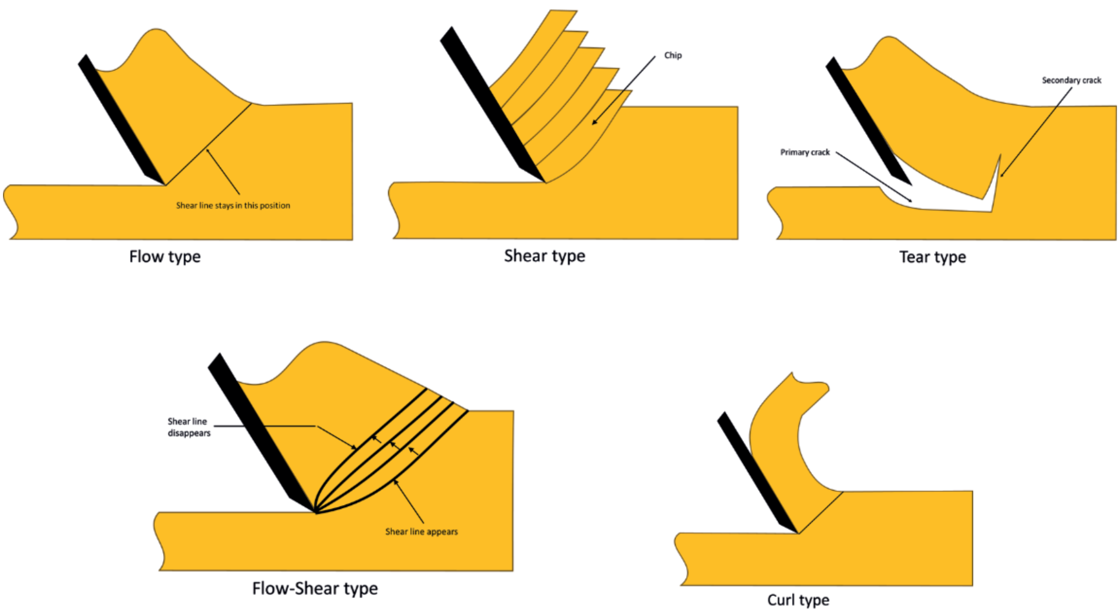

Figure 9. Cutting form types identified in literature (Curl type: Miedema, 1992, others Hatamura and Chiijiwa, 1975)

(Miedema, 1992) gave an indication which cutting type may occur depending on initial cutting depth, see Figure 10.

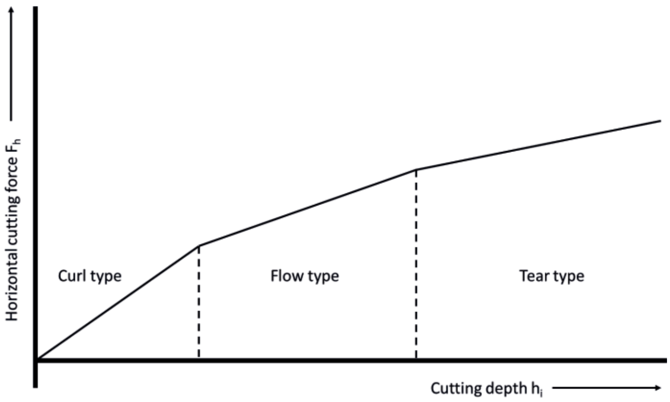

Figure 10. The horizontal cutting force as a function of layer thickness (Miedema, 1992).

From the field of metal working and machining, other cutting types have been identified, which are also recognisable in the dredging industry, see. See Figure 11.

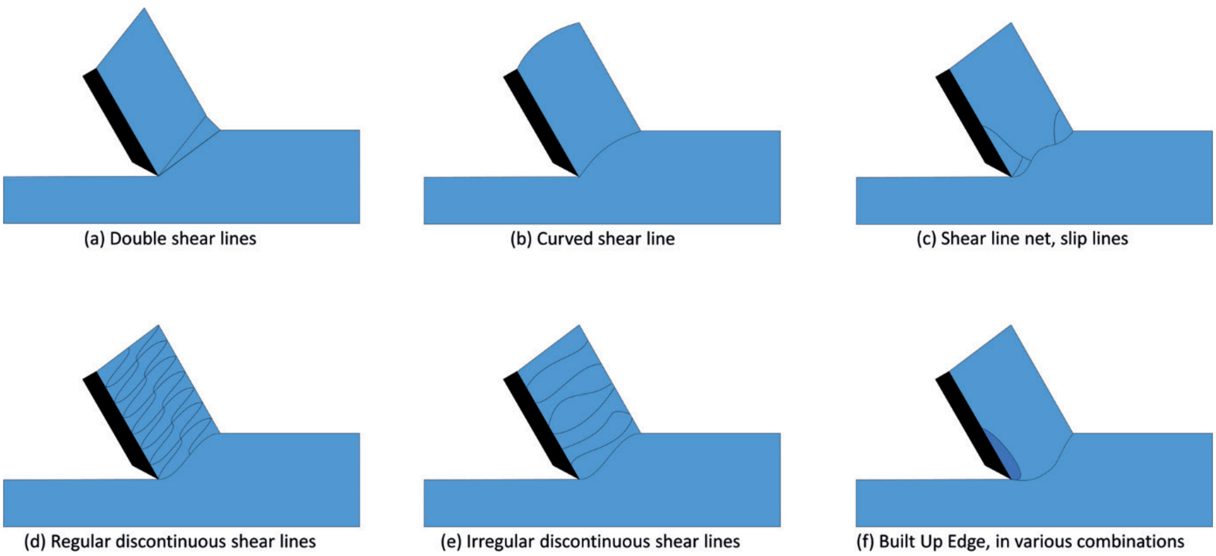

Figure 11. Shear plane modes observed in other materials (a) (Joanknecht and Lobanov, 1980) (b) (Hatamura and Chiijiwa, 1975) (c) (Dewhurst and Collins, 1973) (d) Dewhurst (1978) (e) Dewhurst (1978) (f) (Fang and Dewhurst, 2005)

The shear planes can be either straight or curved and either regular or irregular in form. Each of the phenomena will result in a slightly different chip type. Another complication, well described in metal machining, is a phenomena called the Build Up Edge (BUE) (Fang and Dewhurst, 2005). These are pockets of static material, that cling to the blade and virtually change the geometry of the blade. This phenomenon is known in the dredging industry, as (Miedema, 2014), referred to one form of the BUE as a 'wedge'.

4.1 Involved process parameters

Extensive lists of process parameters for cutting of clay in agricultural fields have been compiled by (Karparvarfard and Rahmanian-Koushkaki, 2015) and (Gebre et al., 2023). For dredging conditions, another interesting list of process parameters for the cutting of rock has been published by (Alvarez Grima et al., 2015). These can be narrowed down by assuming a rigid body motion of a blade through ideal clay in a submerged environment. The various parameters to describe this process can be divided in material properties and operational conditions (see Table 1.).

Table 1. Parameters of material properties and operational conditions. In italic, the properties and conditions used in the Buckingham Π analysis.

Material properties			**Operating conditions**		
Cohesion	c	Pa	*Cutting depth*	h_i	m
Adhesion	a	Pa	*Cutting speed*	v_c	m/s
Shear strength	τ	Pa	*Blade angle*	a	Rad
Plasticity index	PI	%	*Slip line length*	Lsl	m
Liquidity index	LI	%	Blade width	w	m
Density Clay	ρ	kg/m^3	Blade length	L	m
Grain size	d_{50}	m	Shear rate	ε_0	1/s
Gravitational acceleration	g	m/s^2	*Hydrostatic pressure*	p	Pa
Permeability (near infinite small, but might be different microscopically)	k	m/s	Mixture flow	v_m	m/s
Angle of internal friction	α_{in}	rad	Mixture density	ρ_m	kg/m^3
Angle of external friction	α_{ex}	rad	Surface roughness	R_a	m
Fracture speed	v_f	m/s	Plough angle (not applicable, only considering straight cuts)	ι	Rad
			Tip roundness	r_t	m

For some of these parameters, it is useful to have an indication for the range of values occurring for the various types of equipment mentioned in Figure 2. The values in Table 2. are rough estimates probable in the dredging industry and therefore indicative only.

Table 2. Example values for selected parameters

	Cohesion c [kPa]		**Density ρ [kg/m³]**		**Velocity v_c [m/s]**		**Depth h_i [m]**		**Blade length L [m]**	
Equipment	**min**	**max**	**min**	**max**	**min**	**max**	**min**	**max**	**min**	**max**
CSD	15	200	1600	2100	1.57	4.58	0.02	0.10	0.11	0.40
TSHD	5	75	1600	1900	0.13	1.54	0.05	0.50	0.11	0.40
BHD	15	200	1600	2100	0.05	0.50	0.10	1.50	0.50	1.50
BLD	15	200	1600	2100	0.10	1.00	0.10	1.50	0.50	1.50
GD	15	100	1600	1900	0.25	0.50	0.10	1.50	0.50	1.50
AD	5	50	1400	1800	2.00	4.00	0.01	0.30	0.10	0.30
DP	5	75	1600	1900	0.13	1.54	0.01	0.30	0.10	0.30

4.2 Buckingham Π

The important parameters shown in italic listed in Table 1. are used for further analysis. This list can be reduced by elimination of the dependent parameters. This elimination method is called the 'Buckingham Π Theorem', which is used to seek out (dimensionless) groups of parameters that are independent of each other. In this case, the procedure used is as proposed by (Kline, 1986). Percentages and radians do not have a unit, but are not dimensionless (Quincy and Brown, 2016). Hence, they are assigned the dimensions '%' and 'radians'.

It can be noticed that the blade angle is the single parameter in the Table 1. With the dimension radians and will be independent by definition. Arguably, there could be another parameter in radians, e.g. the internal friction angle. Under dredging conditions, the clay might be mixed with sand and the internal friction angle will not be zero. Here, the internal friction angle is considered constant and assumed to be zero. This assumption will not hold for clays with sand content (Jacobs et al., 2005).

In total eleven physical parameters have been identified for the clay cutting process. For these parameters, there are 5 dimensions, see Figure 12.

```
%       c    a   PI   LI   rho  hi   vc   ba   Lsl   L    p
M = [-1   -1    0    0   -3    1    1    0    1    1   -1;    % L
       1    1    0    0    1    0    0    0    0    0    1;    % M
       0    0    1    1    0    0    0    0    0    0    0;    % P
       0    0    0    0    0    0    0    1    0    0    0;    % R
      -2   -2    0    0    0    0   -1    0    0    0   -2];   % T


v = null(M,'r') % solve PI's
M  * v          % Check M*a should be zeros
v' * v          % Check a'*a should be identity for orthogonal kernel
```

Figure 12. Matlab code to calculate Π vectors.

According to Buckingham Π, there should be six dimensionless groups and the execution of the code (see Figure 12.) does result in the following groups.

$$\Pi_1 = \frac{a}{c} \tag{6}$$

This is the adhesion, cohesion ratio important for determining clay behaviour in cutting processes (Chen et al., 2021).

$$\Pi_2 = \frac{LI}{PI} \tag{7}$$

This ratio between Liquidity Index LI and Plasticity Index PI is used to estimate the adherence potential of clay in cutting processes (Thewes, 1999). In a sense, it represents to what extent a clay chip will stick to the blade.

$$\Pi_3 = \frac{\rho}{c v_c^2} \tag{8}$$

This dimensionless group of density ρ, cohesion c and velocity v_c, relates to the shear rate in the material, as it is the only group that contains velocity. For sandy soils, the permeability also includes velocity. For clay the permeability velocity is assumed zero. Though there may be a relation to the ingress of water through the fissures created by the cutting action in a tear type cutting regime. It may show an interesting response to the change from the flow regime to the tear type regime.

A dimensionless group, that is solely depending on the tool used is the blade contact length L over the cutting depth h_i:

$$\Pi_4 = \frac{L}{h_i} \tag{9}$$

When considering the deformation field that arises from the cutting process, there will be some sort of sliding plane where shear will occur. The following ratio is a scale number that relates the deformation field size to the tool size.

$$\Pi_5 = \frac{L_{sl}}{L} :: \frac{L_{sl}}{h_i} \tag{10}$$

However, it can be argued, that the ratio of shear line length L_{sl} to the cutting depth h_i might be a better dimensionless group, as it will better describe the shape of the slip-lines and consequently the type of the deformation and not so much the size of the deformation.

$$\Pi_6 = \frac{p}{c} \tag{11}$$

It is likely that water depth (hydrostatic pressure p) affects the cutting process by restricting tensile failures from occurring (Alvarez Grima et al., 2015; Helmons et al., 2016). Typically a regime change is expected in the range where the hydrostatic pressure is higher than the tensile strength of the material, $p > \sigma_t$. , and in this case there might be a relation to the cohesion c. The blade angle is already a single independent parameter.

4.3 Historical measurements

Over the course of time, there have been several experiments with the cutting of clay. In which a wide variety in geometries and conditions have been applied. Here, an attempt is made to uniformly evaluate the public results with the above independent (dimensionless) groups. The geometries and the setup require some explanation before they can compared.

Table 3. Overview of publications about the cutting of clay

ID	Publication	Set up	Condition	Dimension
1	Hatamura and Chijiiwa (1976)	Standard	Dry	2D
2a 2b	Joanknecht and Lobanov (1980)	Chamfered, serrated blade Same, but different pattern	Submerged	3D
3	Stam (1983)	Double action	Submerged	2D
4	Miedema* (1992)	Double action	Submerged	2D

*Miedema refers to Stam, but there are slight differences in their presentations.

All data sets from Table 3. have been compiled in Figure 13. (Hatamura and Chijiiwa, 1976) conducted two different experiments. A series of small scale preliminary tests to identify cutting phenomena and a series of larger experiments where actual parameters were measured. Both experiments were conducted under dry conditions, similar to road building operations. Elementary, they used a straight sharp blade that was pushed linearly through plastic loam. Parameters tested were blade angle, cutting depth and cutting velocity.

(Joanknecht and Lobanov, 1980) investigated methods to prevent clay from sticking to the blade. As a solution, the blade was designed with two facetted surfaces. One small chamfer was in contact with the clay and the long side surface of the blade was not in contact with the clay. The idea was that the clay was pushed away by the chamfer and curled over the blade into the suction mouth. The stated blade angle by (Joanknecht and Lobanov, 1980) refer to the angle of the blade and as such only to the side surface. The chamfer itself had a different angle and that was used as the cutting angle here. Furthermore, the blades were serrated to facilitate further brake up of the cut material. This will also influence the measured cutting forces.

(Stam, 1983) performed a series of tests, which were part of research in finding an optimal clay cutting tool. The setup used two parallel straight blades at different heights, each cutting half of the total cutting depth. In order to fit this in a uniform assessment of conditions, the blade is considered as one blade with double the width. As such, the measured horizontal cutting force is distributed evenly of the blade edge.

(Miedema, 1992) did not conduct any experiments himself, but referred to various other publications to validate his model. As such, he presents a graph with measurements of (Stam, 1983), that appear to be similar, but in detail does have slightly different data points. For reviewing his information, the same modification as for (Stam, 1983) has been applied. Similarly, (Schrieck, 1996) is using the same dataset of (Stam, 1983) for model validation.

Remarkably, the models by (Schrieck, 1996) and (Miedema, 1992) are off by a factor of 2 (see Figure 13). This has been fleetingly mentioned by (Miedema, 1992), but not conclusively addressed. Apparently, there is an assumption in the model that is not reflected in practice.

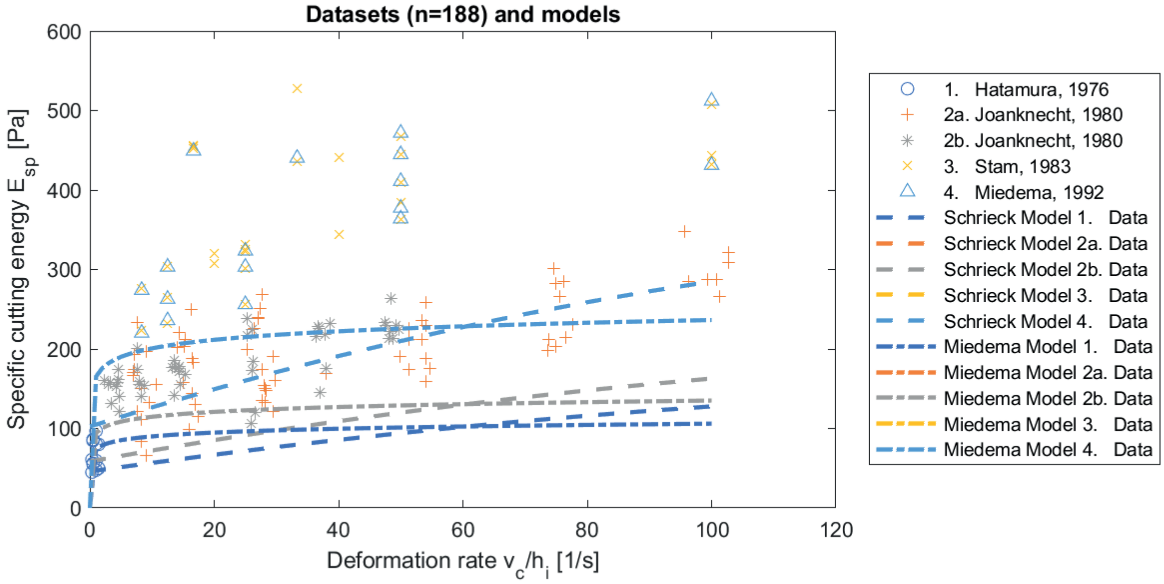

Figure 13. Overview of available experiments and models.

Another evaluation which may be made is, whether the models and the measurements are covering the range of working conditions of the equipment mentioned in Table 2. On the same horizontal axis, the various equipment has been placed according to their operating range see Figure 14.

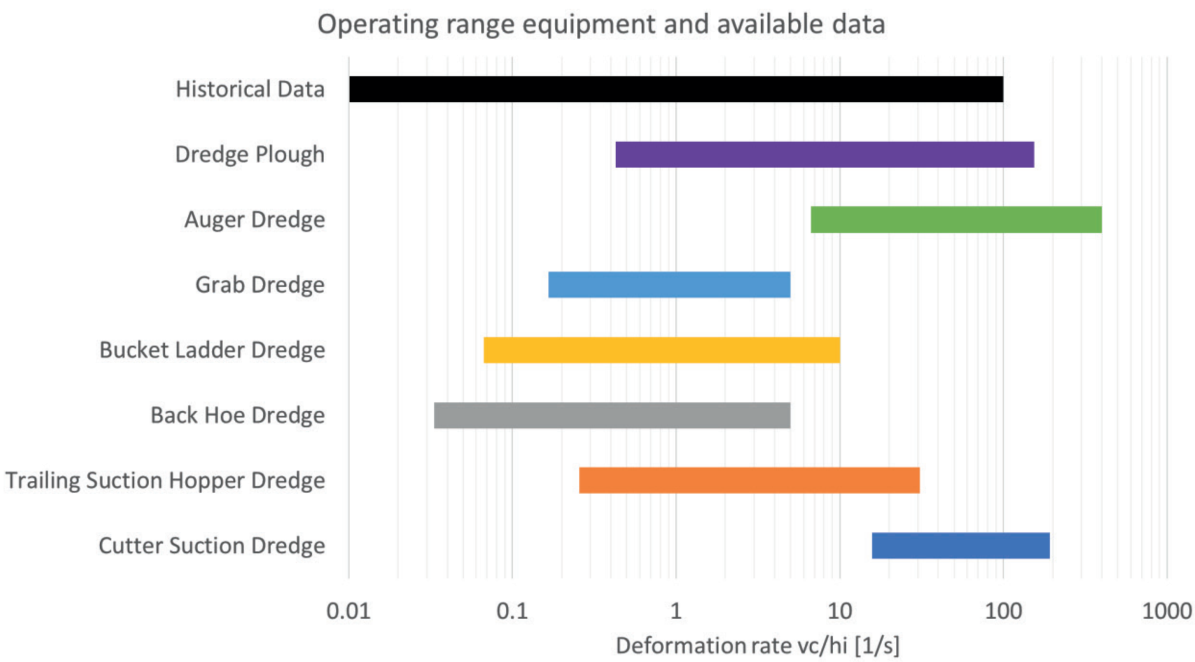

Figure 14. Operating range equipment and available data for deformation rate

According to the diagram in Figure 14., the deformation rate, as encountered in the various types of equipment, is indeed covered by the available experimental data. Any differences between the models and the data might be due to a different behaviour than described by the models. However, this is not very clear from the available literature, as the cutting behaviour is not very well described.

4.4 Deformation Mechanisms Map

Similarly to Figure 10., where the cutting behaviour is classified to the horizontal cutting force depending on the cutting depth, now also the dimensionless velocity group can be used as a parameter for exploring the other observed cutting types. By combining the two parameters for cutting depth and the velocity results in a deformation mechanisms map, see Figure 15. The resulting parameter in z-axis is the specific energy consumed by the process that is made dimensionless by dividing with the cohesion, in a similar fashion as (Schrieck, 1995) and (Miedema, 1992) have done in Figure 6. and Figure 7.

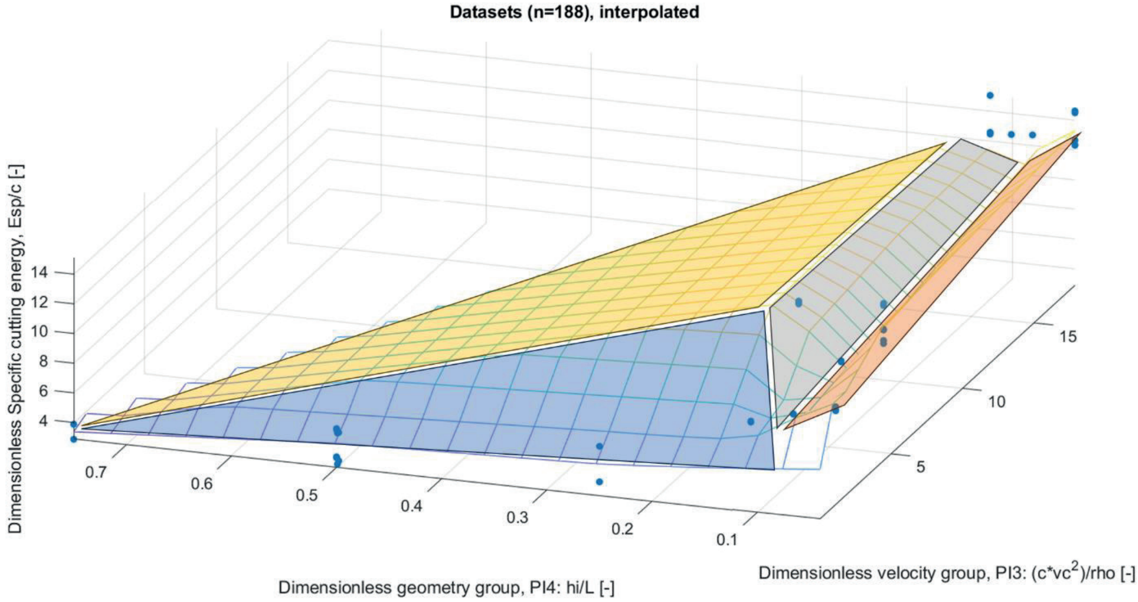

Figure 15. Landscape of unified cutting test data

The landscape on the map indicates the different cutting types. The data points are too few to identify the types conclusively. At very low speeds, there is a decreasing specific cutting energy for an increasing cutting depth. For the velocity range, there appears a trough around the very small cutting depths.

Furthermore, this map, of available data and resulting behaviour, could be compared with the range of operating conditions of the various equipment from Figure 2. The available data has been mapped on the dimensionless parameters Π_3 and Π_4 for velocity and geometry in Figure 16.

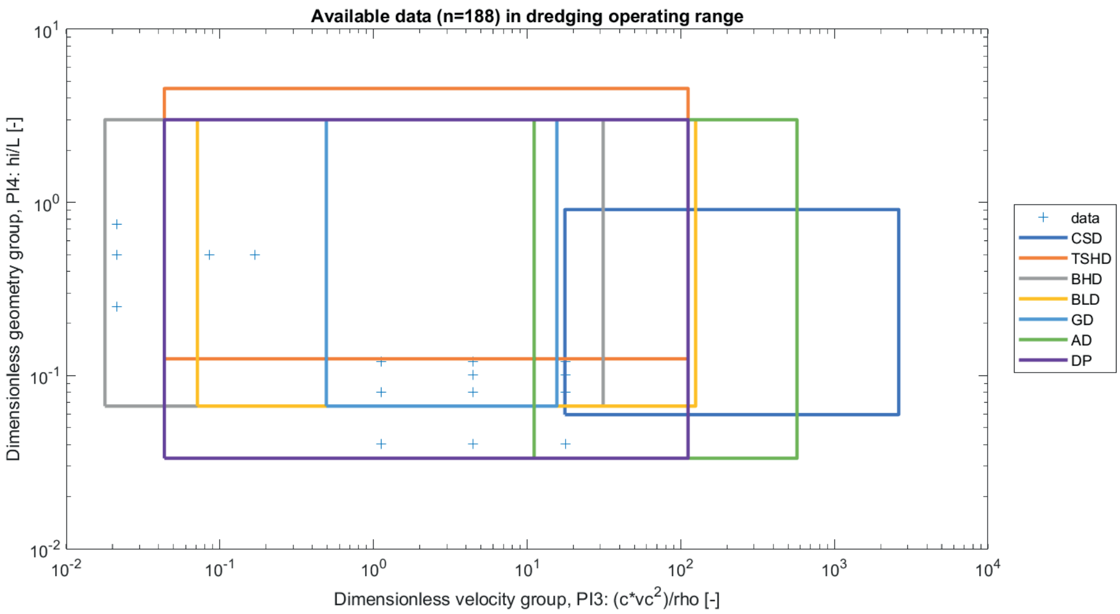

Figure 16. Operating range equipment and available data for dimensionless parameters.

Apparently, the available data does not cover the operating range of dredging equipment in the dimensionless parameter space. Only the fully mechanical dredges are partially explored. Although the experiments from (Stam, 1983) and (Joanknecht and Lobanov, 1980) were specifically designed for TSHD operation, they only cover a small corner of the dimensionless operating range. Especially CSD operation is poorly explored. The diagram of Figure 16. is useful for designing additional experiments to uncover the mechanisms of clay cutting in dredging practice.

5 CONCLUSION

This literature review shows several methods to improve the understanding of the cutting processes in clay. Conclusions to be drawn from the presented publications are:

- The plastic behaviour of clay during cutting is more complicated than a single shear plane at which the shear stress is acting. Usually the shear plane comprises at least a curved surface, but could also be multiple shear planes in a deformation field. These additional shear planes contribute to the overall required cutting forces and may explain the differences with the straightforward models and the measured data, identified in Figure 13. and mentioned by Miedema. Possible descriptions that may be useful to refine the model, may be the slip line method developed by (Dewhurst and Collins, 1973) and alluded to by (Schoonbeek et al., 2006). Generally, they find more, and more complex slip lines than just one straight shear line.
- The resistance of a material against plastic deformation is due to shear stresses on the shear planes. There are various models to describe shear stress related to the shear rate occurring. The rate process theory is an accepted accurate model, but is limited in its ability to account for the special material properties of clay. Especially interesting is the Composite Dilatancy model as it is capable of handling transient and off-plane influences as porewater movement moreover the model is fast.
- The Buckingham Π method provides dimensionless parameter groups which can be used to summarize experimental results from different setups. It can also be used to evaluate the performance of cutting process describing models and correlate these with available measurements.
- Although there has been an extensive investigation in the cutting process for the whole range of deformation rates as encountered in dredging practice, it is less so covering the range expressed in the dimensionless parameter groups for cutting depth and cutting speed. The not investigated range may have important information that describes the cutting behaviour for certain widely used dredging equipment, especially the Cutter Suction Dredge.
- When setting up new experiments in the laboratory or in the field, the experiments should focus on areas not yet covered in the domain for dimensionless speed and depth. Additionally, experiments should focus on recording the observed behaviour under these testing conditions.

These conclusions will be the starting point for the ensuing model derivation phase and in the validation phase in the rest of the project.

ACKNOWLEDGEMENTS

This PhD. research project was initiated by Damen to investigate the rapid plastic deformation in the Cutting of Highly Plastic Soils (CHiPS). Many thanks go to Hendrik Jan de Kluiver for facilitating this research within Damen. Cees van Rhee has to be mentioned as he accepted my proposal for this PhD project and was invaluable for his advice to follow this particular line of research. It is a tragedy he will not be able to see the results of my work.

LIST OF SYMBOLS

AD	Auger Dredge
BHD	Back Hoe Dredge
BLD	Bucket Ladder Dredge
BUE	Built Up Edge
CEDA	Central Dredging Association

CHiPS	Cutting Highly Plastic Soils
CSD	Cutter Suction Dredge
DP	Dredge Plough
GD	Grab Dredge
PIANC	Permanent International Association of Navigation Congresses
TSHD	Trailing Suction Hopper Dredge
VBKO	Vereniging Bedrijven in Kust- en Oeverwerken (Currently: Vereniging van Waterbouwers)
VOUB	Voortgezette Opleiding Uitvoering Baggerwerken
WID	Water Injection Dredge

α	rad	Blade Angle (ba in Matlab)
α_{in}	rad	Angle of internal friction
α_{ex}	rad	Angle of external friction
β	rad	angle of the shear plane
$\dot{\varepsilon}_0$	1/s	Shear rate
ι	rad	Plough angle
λ	m	Distance between equilibrium points
λ_s	-	Strain rate factor
ϱ_{t0}	mol/s	Reaction rate at temperature T_0
ϱ_{t1}	mol/s	Reaction rate at temperature T_1
Π_1	-	Pi group 1: adhesion, cohesion ratio
Π_2	-	Pi group 2: adherence potential
Π_3	-	Pi group 3: shear rate number
Π_4	-	Pi group 4: tool / cutting depth ratio
Π_5	-	Pi group 5: slip line geometry parameter
Π_6	-	Pi group 6: hydrostatic pressure ratio
ρ	kg/m³	Density
ρ_m	kg/m³	Mixture density
τ	Pa	Shear Stress

a	Pa	Adhesion
c	Pa	Cohesion
d_{50}	m	Mean grain size diameter
E_a	J	Activation Energy
E_{sp}	Pa	Specific Cutting Energy
F_h	N	Horizontal Cutting Force
F_v	N	Vertical Cutting Force
g	m/s²	Gravitational Acceleration (9.81 m/s²)
h	Js	Planck Constant ($6.626 \cdot 10^{-34}$ Js)
h_b	m	Blade height
h_i	m	Initial cutting height
k	J/K	Boltzmann Constant ($1.3807 \cdot 10^{-23}$ J/K)
k	m/s	Permeability
L	m	Blade length
LI	%	Liquidity Index
LL	%	Liquid Limit
L_{sl}	m	Length of the slip lines
n	-	Sample size
N	1/mol	Avogadro constant ($6.02 \cdot 10^{23}$ 1/mol)
PI	%	Plasticity Index
PL	%	Plastic Limit
q	J	Heat consumption for reaction
r_t	m	Tip roundness
R	J/mol/K	Universal gas constant (8.314 J/mol/K)
R_a	m	Surface roughness
S	1/m²	Number of bonds per unit area

t	s	Time
T	K	Temperature
T_0	K	Initial temperature
T_1	K	Terminal temperature
v_c	m/s	Cutting Velocity
v_f	m/s	Fracture speed
w	m	Blade width
X	-	Barrier crossing function

REFERENCES

Alvarez Grima M., Miedema S.A., Ketterij R.G. van de, Yenigül N.B., and Rhee C. van (2015). Effect of high hyperbaric pressure on rock cutting process *Engineering Geology* 196 (2015) 24–36; Elsevier; doi: 10.1016/j.enggeo.2015.06.016

Arrhenius S. (1889). Über die Reaktionsgeschwindigkeit bei der Inversion von Rohrzucker durch Säuren *Zeitschrift für Physikalische Chemie* 4 226-48; (1889); Zenodo; doi:10.1515/zpch-1889-0416

Burger M. den (2003).Mixture Forming Processes in Dredge Cutter Heads *PhD Thesis*; TU Delft

CEDA/IADC (2018). Ch.5 Equipment and methods *Dredging for Sustainable Infrastructure*; CEDA/IADC; The Hague; ISBN 978-90-9031318-4

Chen X., Broecke J. van den, Liu G., Hong G. and Miedema S.A. (2021). Experimental study on the adhesion factor of clay *Terra et Aqua* #163 Summer 2021; IADC; The Hague

Dewhurst P. and Collins I.F. (1973). A matrix technique for constructing slip-line field solutions to a class of plane strain plasticity problems *International Journal for Numerical Methods in Engineering*, Vol. 7,357-378 (1973); John Wiley & Sons, Ltd.

Dewhurst P. (1978). On the Non-Uniqueness of the Machining Process *Proceedings of the Royal Society of London. Series A. Mathematical and Physical Sciences, Apr. 19, 1978,* Vol 360. No. 1703 (Apr. 19, 1978), pp. 587-610; Royal Society

Fang N. and Dewhurst P. (2005). Slip-line modelling of built-up edge formation in machining *International Journal of Mechanical Sciences* 47 (2005) 1079-1098; Elsevier

Gebre T., Abdi Z., Wako A. and Yitbarek T. (2023). Development of a mathematical model for determining the draft force of ard plow in silt clay soil *Journal of Terramechanics* 106 (2023) 13–19; Elsevier; doi 10.1016/j.jterra.2022.11.004

Glasstone S., Leidler K.J. and Eyring H. (1941). The Theory of Rate Processes, The Kinetics of Chemical Reactions, Viscosity, Diffusion and Electrochemical Phenomena *International Chemical Series*, 1941; Mcgraw-Hill Book Compagny, New York, N.Y.; OCLC: 473894177

Hampel A. and Schulze O. (2007).; The Composite Dilatancy Model: A constitutive model for the mechanical behavior of rock salt *The Mechanical Behavior of Salt – Understanding of THMC Processes in Salt*; CRC Press

Hatamura Y. and Chijiiwa K. (1975). Analysis of the mechanism of soil cutting (1st report, Cutting patterns of soils) *Bulletin of the JSME*, Vol. 18, No. 120, June, 1975; doi: 10.1299/jsme1958.18.619

Hatamura Y. and Chijiiwa K. (1976). Analysis of the mechanism of soil cutting (3rd report, Distribution of stresses on cutting bade and cutting force) *Bulletin of the JSME*, Vol. 19, No. 137, November, 1976; doi: 10.1299/jsme1958.19.1376

Helmons R.L.J., Miedema S.A., Alvarez Grima M. and Rhee C. van (2016). Modelling fluid pressure effects when cutting saturated rock *Engineering Geology* Volume 211, 23 August 2016, Pages 50-60; Elsevier; doi: 10.1016/j.enggeo.2016.06.019

Hoff J. van 't and Kolff A.N. van der (2012). Ch. 9 Special fill materials and problematic subsoils *Hydraulic Fill Manual for Dredging and Reclamation Works*; CRC Press; ISBN 978-0-415-69844-3

ISO 17892 (2018). Part 12: Determination of liquid and plastic limits; *Geotechnical investigation and testing - Laboratory testing of soil* (ISO 17892-12:2018,IDT)

Jacobs W., Kesteren W. van and Winterwerp J.C. (2005). Ch. 8. Strength of sediment mixtures as a function of sand content and clay mineralogy *Sediment and Ecohydraulics: INTERCOH 2005*, p.91-107; Elsevier; doi: 10.1016/S1568-2692(08)80010-1

Joanknecht L.W.F. and Lobanov V.A. (1980). Linear cutting tests in clay *Third International Symposium on Dredging Technology*, paper E2, p.315-332; BHRA Fluid Engineering, Cranfield, Bradford

Karparvarfard S.H. and Rahmanian-Koushkaki H. (2015). Development of a fuel consumption equation: Test case for a tractor chisel-ploughing in a clay loam soil *Biosystems Engineering* 130, February 2015, 23-33; Elsevier; doi: 10.1016/j.biosystemseng.2014.11.015

Kline S.J. (1986). Ch. 2. Dimensional Analysis and the Pi Theorem Units and Dimensions *Similitude and Approximation Theory*, pp.8-35; ISBN 978-0-387-16518-9

Meng Z., Mingchao L., Zhang Y. and Che, C.Q. (2020). Multi-step deformation mechanical metamaterials *Journal of the Mechanics and Physics of Solids* 144 (2020) 104095

Merchant M.E. (1945). Mechanics of the Metal Cutting Process. I. Orthogonal Cutting and a Type 2 Chip *Journal of Applied Physics*, 16, 267 (1945); doi: 10.1063/1.1707586

Meshkati E., Talmon A., Luger D. and Bezuijen A. (2021). Rheology of clay rich soft sediments: from liquid to geo-mechanics *Proceedings of the CEDA Dredging Days 2021*; Rotterdam

Miedema S.A. (1992). New Developments Of Cutting Theories With Respect To Dredging The Cutting Of Clay; *Proceedings WODCON XIII*; Bombay

Miedema S.A. (2014). The Delft Sand, Clay & Rock Cutting Model *Textbook*; (2014); doi: 10.3233/978-1-61499-454-1-i

PIANC (2016). Classification of Soils and Rocks for the Maritime Dredging Process *PIANC Report No. 144* - C.2.1 Trailing Suction Hopper Dredger; ISBN 978-2-87223-222-2

Quincey P. and Brown R.J.C. (2016). Implications of adopting plane angle as a base quantity in the SI *Metrologia*, Volume 53, Number 3, p. 998; doi: 10.1088/0026-1394/53/3/998

Schoonbeek I.S.S., Kesteren W.G.M. van, Xin M.X. and Been K. (2006). Slip Line Field Solutions As an Approach to Understand Ice Subgouge Deformation Patterns *Proceedings Of The Sixteenth International Offshore and Polar Engineering Conference*

Schrieck G.L.M. van der (1996). Ch. 4.3 Snijden van klei *Collegedictaat f14: Baggertechniek*; (1996)

Schrieck G.L.M. van der (2014). Ch 4.3 Cutting Clay *Lecture Notes Master Course CIE5300*, Dredging Technology Book 1 special edition WODCON XXII 2022

Stam P.T. (1983). Analyse ten behoeve van het ontwerp van een klei snijdende sleepkop *Report: CO/82/129* TU Delft

Volker L.G. (1947). Hfd. VIII De productie en de exploitatie van zuigers *Baggermaterieel, Constructie en Gebruik*

VOUB (1998). Materieelinzet en productieraming *Voortgezette Opleiding Uitvoering Baggerwerken, deel 10*; ISBN 90-9011108-5

Werkhoven J.J., Nieuwboer B.J., Louis A.A., Ramsdell R.C. and Miedema S.A. (2018). A pseudo-analytical model for CSD spillage due to rotational velocity-induced flow *Proceedings of the Western Dredging Association Dredging Summit & Expo '18*